An Investigation of Object Shadows Utilization In 3D Shape Re-Construction Using Inexpensive Equipment

Dr. Ghassan A. Al-Kindi * & Dr. Ali Abbar Khleif **

Received on:1/6/2009
Accepted on:5/11/2009

Abstract

An approach for automatic 3D object re-construction using its shadow is presented. The approach investigates the use of information inherited by the generated object shadows to re-construct the object geometry. An algorithm is developed that make use of object height information for the directions associated with the incident light and the generated object shadows, hence, acquired height features represents the object features that have actually obstructed the incident light. The technique is tested using objects of different shapes. Close to real measurements are gained and the overall accuracy of the system is found to be within 0.75 mm using the adopted imaging hardware and setup. Obtained results confirmed the validity of the proposed approach.

Keywords: CAD/CAM, 3D object Re-construction, Robot vision applications.

إستقصاء بيانات ظلال الأجزاء لإعادة بناء الشكل الثلاثي الأبعاد بأستخدام معدات رخيصة الثمن

الخلاصة

في هذا البحث تم تقديم خطوة نحو عملية إعادة بناء الأجزاء ثلاثية الأبعاد ذاتياً بأستخدام ظلال هذه الأجزاء. حيث تعتمد هذه الخطوة على استكشاف وأستخدام المعلومات المتأصلة في الظلال المتولدة للأجزاء من أجل إعادة بناء الشكل الهندسي لهذه الأجزاء. تم تطوير خوارزمية تعمل على الأستفادة من بيانات إرتفاع الجزء في الأتجاهات ذات العلاقة بالضوء الساقط وظلال الجزء المتولدة، حيث أن سمات الجزء المتولدة تمثل السمات التي تقاطع أو تعرقل إتجاه الضوء الساقط. تم أختبار التقنية على عدد من الأجزاء مختلفة الأشكال، وكانت النتائج قريبة من الواقع بدقة مقدارها 0.75 ملم بأستخدام المكونات المادية والتهيأة لنظام الرؤية المعتمد في هذا البحث، كما أظهرت النتائج المستحصلة صحة المنهجية المقترحة.

***Mechanical Engineering Department, University of Technology/Baghdad**
**** Production and Metallurgy Engineering Department, University of Technology/ Baghdad**

Introduction

One of the main challenges in modern machine vision is to develop techniques that are inexpensive, fast and accurate, can handle objects with arbitrary appearance and need little or no user intervention [1].

It is often the case that users create 3D object models using Computer Aided Design (CAD), however CAD systems require highly trained professional users and usually takes much time to create complicated models, hence they present a bottleneck in real applications [2]. Alternatively, vision-based techniques to obtain 3D object model data automatically by observing real objects may establish a beneficial solution that is of great significant in reverse engineering applications.

Application of 3D object reconstruction has been set as the common focus of many published articles. Daum and Dudek [3] used the geometry of cast shadows to re-construct scene structure. Their approach is based on collecting a set of images from a fixed viewpoint while a known light source moves. By observing how the shadows move as a function of the light source position, the three-dimensional structure of the scene is recovered. Braquelaire and Kerautret [4 and 5] proposed two methods for surface re-construction from image shading. Both methods are based on the propagation of geometric features along the re-constructed discrete surface. Kerautret [6] presented an approach to recover the shape from a single image. A novel definition of patches was introduced in his work to overcome the concave/convex ambiguity when only one image is used for the re-construction. Savaresez et al [7] presented a "shadow carving" technique for 3D object re-construction that makes use of minimal and inexpensive equipment. Yu and Chang [8] presented alternative shadow-based method for recovering high-frequency surface geometric details. Other methods for 3D surface reconstruction include "shape-from-shading" [9] that only takes one input image and heavily relies on the regularization term, though recovered surfaces often have obvious errors [10]. Photometric stereo [11] can improve on this by using multi images.

The main goal of this paper is to investigate the feasibility of 3D object re-construction by using object's shadows, generated by controlled incident light. A technique is proposed and applied to evaluate its potential in the 3D reconstruction of objects. It is worth noting that the technique is meant to acquire objects height attributes which are not directly visible to the camera; however, the technique is valid only to acquire object height features in the directions associated with the generated shadows. Hence, acquired height features represent the object features that have actually obstructed the incident light. Future application areas of the technique may include the eye-in-hand Robot field to beneficially increase the perception level available for the imaging system, the dimensional measurement of manufactured parts,

and the area of reverse engineering utilizing CAD/CAM systems.

Hardware Setup

An Epson PC-500 type camera is used to acquire the images of this work. A single light source is used and set in an oblique direction relative to the horizon and only parallel light rays are assumed to intercept the object. Reflected light is then reaching the camera due to the diffused reflection phenomena, where adequate intensity is gained. Figure (1) shows the system set-up used in this work, whereas Figure (2) represents the symbols employed in the proposed technique. The perpendicular distance between the light source and the base line is denoted by (l), while the distance between the object edge and the light source along the base line is denoted by (d). The symbols (h), (w), and (s) represent the object height, width, and shadow length, respectively.

Proposed 3D Shape Re-Construction Technique

The proposed technique acquires 3D features of the object using a single image. Figure (3) represents a flow chart of the technique. Top view of the object is captured using oblique direction of illumination; Figure (4.a) shows an example of a 10mm height block gauge object which was acquired with oblique illumination where the camera height (c) was set to 150 mm, the light height (l) was set to 190 mm and the light distance from the object (d) was 150 mm. Two versions of the single input image are created by processing of the acquired image data. The first is the ***Shadow Image*** that is achieved by converting the image data into a binary image presentation by using an appropriate threshold value to extract the block gauge shadows; Figure (4.b) represents the obtained ***Shadow Image*** of the block gauge component that is presented in Figure (4.a).

The second version of the image is the ***Object Image*** that is created by eliminating shadow information using a suitable threshold value to enable the detection of the object features. Both Length and width data attributes of the object are then extracted easily from this version of the image; the methodology presented in [12] was adopted to achieve this task using the calibration model gained in this work. Figure (5.a) represents an example of an image of the same block gauge component that is acquired using ambient lighting, whereas Figure (5.b) represents results of the acquired ***Object Image*** of the same block gauge component. Both resulting images are used to obtain object attributes by using a suggested technique.

The suggested technique of object height recovery is based on the trigonometric relationships of a right triangle. The technique determines the height of an object from a number of known parameters, see Figure (2).

The relationship formulation of similar triangles could yield the followings:

$$h = \frac{l \times s}{d + w + s} \qquad \ldots\ldots\ldots (1)$$

Both the ***object*** and ***shadow images*** are then subjected to further

processing to obtain 3D shape re-construction by computing local heights at each object pixel location.

Figure (6) shows results of the 3D object re-construction of the block gauge using the proposed method.

Image Calibration

The images in this work are calibrated to achieve required dimensional presentation. The calibration was achieved using the top view of a circular object of (25 mm) diameter. A set of images obtained using different camera heights. Each image is then processed to obtain the average diameter of the circular component in pixel units. Therefore, the actual object diameter is compared to the extracted diameters; results are presented in Figure (7). The mathematical presentation of the equation that best fits the acquired results is given by:

$$c = 0.0083s^2 - 3.4s + 450 \quad \ldots\ldots \quad (2)$$

Where (c) presents the physical camera height in mm units and (s) presents acquired entity length within the image in pixel units.

To evaluate the assumed case of that only parallel rays of light intercepts the object, a set of experimental tests was conducted. A block gauge of (10 mm) height is captured using a camera height (c) of 150 mm. Different light positions (p) along a line that is inclined from the horizon by 45^o are used in the range of 140 mm to 160 mm. The object shadow length (s) is extracted from each setting case. The mathematical presentation that best fits the acquired results is given by:

$$\Delta s = 0.05\, l - 1.9 \quad \ldots\ldots \quad (3)$$

Where (Δs) present the expected difference of the shadow length (s) in pixel units and (l) presents the employed light position in mm units. According to the obtained results, the diverted lighting angle α is less than (1.5°), hence is small and could be neglected.

In another evaluation test both camera height (c) and light source height (l) and distance (d) were fixed to (150 mm), however a number of objects having different object heights (h) were used. Figure (8) shows acquired results, where linear relationship is obtained that could be expressed by the following equation:

$$h = 0.18s + 0.168 \quad \ldots\ldots \quad (4)$$

Where (h) is the object height and s is the resulting shadow length using the camera height, light distance and light heights of 150 mm each.

Experimental Results and Evaluation

To assess the potential of the proposed algorithm further investigation was carried out using different object shapes. The aim is to highlight any problem areas that encounter the execution of the proposed algorithm and to evaluate the accuracy level that could be achieved in real applications. All conducted tests were repeated 5 times and acquired results showed to be close; hence an example is given bellow for each type of tests to demonstrate the quality of gained results.

A tapered wooden object was used, Figure (9). Figure (10) demonstrates the extracted component features for the 3D re-construction task. The resulting shape matches the original object shape to a certain degree of accuracy.

Minor shape defects could be noticed in the resulting object height attributes due to the sampling criteria employed. The overall result of this test extends the applicability of the developed methodology to inclined surfaces.

In an extended test a cam component that has a more complicated curvature shape is considered, Figure (11). Accordingly, the acquired images were processed and Figure (12) shows the extracted length, width and height attributes from the image using the proposed methodology. Results of this case have also demonstrated that the proposed method is readily applicable to complicated curvature shape objects. The resulting shape has very close to real features. Only minor defects may be recognized that could be attributed to the limited adopted resolution of the imaging system.

A more challenging case was also considered where a dome shape component was used, Figure (13). Figure (14.a) and (14.b) demonstrates the extracted length and width attributes of the dome component respectively. Both sets of attributes indicate symmetrical distribution of the points around the component central axis to denote a circular section.

Figure (14.c) shows the height attributes of the dome object extracted from shadow data. This figure also indicates the well recognition of the original object height features using the developed methodology. Figure (14.d) shows an acceptable surface profile that is approximately similar to the real dome shape component. This view is adequately obtained because it is viewed from a point that is perpendicular to the light source point. The re-constructed top view of the dome component, figure (14.e) shows insufficient object information at both left and right sides of the component top view. This is due to the use of a single captured image affected by a unidirectional parallel ray light source. Accordingly, the re-construction of 3D dome shape component, figure (14.f) has resulted acceptable shape in the related viewing direction only. Therefore, it is required for such cases to acquire an additional image with different lighting direction to satisfy the system requirement and to enable the extraction of more accurate dimensions of the object. This case therefore, could be stated as a system limitation point to achieve 3D re-construction of the object profile based on the developed methodology using a single image.

To demonstrate further limitation of the proposed methodology, a rectangular-section rod with two perpendicular grooves cut in its top surface was used in the investigation, Figure (15.a). The light source was set in an inclined angle but with a parallel direction to the first groove. Obtained results, Figures (15.b) and (15.c), show that the proposed methodology succeeded to provide the shape attributes of the object, however, only for the direction associated with the incident light and the generated object shadow. Figure (15.d) represents the acquired 3D reconstruction of the object, where it is obvious from this figure that only

the first groove was recovered in the object shape, whereas the second groove was completely missed out due to the employed lighting direction. The second groove did not obstruct the incident light and therefore the formed shadow does not inherit any information regarding its shape. To overcome this limitation, additional images of the object with different lighting directions are required so that the formed shadows inherit all possible features of the object shape.

Table (1) lists the real physical dimensions of the objects used in the investigation. The computed dimensions based on the proposed methodology of these objects and related resulting errors of measurements are also included for comparison and clarity.

Resulting errors of measurements of the block gauge component indicate that the maximum difference between the computed dimensions and the real physical dimensions is less than 0.65 mm which is occurred in the length attribute set. While for the tapered shape component the maximum error is found to be in the height attribute set of a value less than 0.74 mm. However, for the cam component the maximum error was found to be 0.68 mm in the object length attribute set. The dome shape component showed to have closer tolerances in the valid directions of measurements, a maximum error of less than 0.55 mm is recorded within the object length attribute set. Close to real measurements were also obtained using the rectangular-section rod. Maximum error of less than 0.45 mm was provided for the object attributes; however, no shape information regarding the second groove of the object was gained.

These minor object distortions and measurement inaccuracies especially at points close to the object boundary were obtained due to the employed imaging resolution, image threshold value used and the approximation used in the calibration process. It could be noted that points close to the object boundary are more prone to false feature extraction than the points inside the object surface area. However the overall acquired results indicate that the proposed attribute extraction process is valid and could yield close to real dimensional measurements of the components under test within an accuracy of 0.75 mm using the adopted system hardware. Though, to generalize this finding to other system hardware, care should be given to the calibration task and proper selection of image threshold value must be achieved to enable valid processing of image data and accepted extraction of object attributes.

Conclusions

Although the goal of re-constructing 3D objects from a single captured image is a challenging problem, the suggested methodology succeeded to achieve close to real measurements of different object shapes. However, the proposed methodology suffers from a defined limitation that it can recover object features only for the directions associated with the incident light and the generated object shadows. Object features that do not fulfill the obstruction of light

are therefore un-recoverable using this methodology. Hence, additional images of the object with different light position would enhance the recovery of these features.

Results of the conducted experiments showed that the proposed algorithm is capable within the accuracy limit of the system to generate 3D re-construction of objects. The overall accuracy of the system was found to be within 0.75 mm using the achieved setup and the adopted imaging hardware. Results also showed that the system is applicable to handle different shape objects including those having various changes in materials, colors, heights, and sizes. These close to actual measurements were gained due to the well control of light, suitable selected image threshold value, and the careful setting of calibration. Hence to generalize this work findings fulfillment of the equipment setup, calibration and processing must be maintained.

Based on the conducted experiments, it can be observed that the points close to the object boundary are more prone to false feature extraction than the points inside the object surface area due to the image quality and the selected value of image threshold. These erroneous points may have a cumulative effect on the feature attribute assignment process and therefore may affect the process of 3D re-construction.

References

[1] Martin C. M., "*Genetic programming for real world robot vision*" IEEE International Conference on Intelligent Robots and Systems, Vol. 1, 2002, pp. 67-72.

[2] Page D., Koschan A., Voisin S., Ali N. and Abidi M."*3D CAD model generation of mechanical parts using coded-pattern projection and laser triangulation systems*" Assembly Automation, Vol. 25 · No. 3, 2005, pp. 230–238.

[3] Daum M. and Dudek G. "*On 3-D surface reconstruction using shape from shadows*" Proceedings 1998 IEEE Computer Society Conference on Computer Vision and Pattern Recognition, 1998, pp. 461-468.

[4] Braquelaire A. and Kerautret B., "*Reconstruction of discrete surfaces from shading images by propagation of geometric features*" Discrete Geometry for Computer Imagery, volume 2886 of LNCS, Springer, Berlin, 2003, pp. 257–266.

[5] Braquelaire A. and Kerautret B. "*Reconstruction of Lambertian surfaces by discrete equal height contours and regions propagation*" Image and Vision Computing Vol. 23, 2005, 177–189.

[6] Kerautret B, "*A Robust Discrete Approach for Shape from Shading and Photometric Stereo*", Internal Report, Laboratoire Bordelais de Recherche en Informatique, Universite

Bordeaux, Talence, France, 2004.

[7] Savaresez S., Rushmeier H., Bernardiniy F. and Peronaz P. "*Implementation of a Shadow Carving System for Shape Capture*" IEEE computer society, Proceedings of the First International Symposium on 3D Data Processing Visualization and Transmission 2002, pp. 12-23.

[8] Yu Y., and Chang J., "*Shadow Graphs and 3D Texture Reconstruction*", International Journal of Computer Vision, Springer Science, Vol. 62, No.1-2, April-May 2005, pp. 35-60.

[9] Horn B. and Brooks M. "*The Variational Approach to Shape from Shading*", Computer Vision, Graphics & Image Processing, Vol. 33, 1986, pp.174–208.

[10] Al-Kindi G., Baul R. and Gill K. "*Experimental Evaluation of 'Shape from Shading' for Engineering Component Profile Measurement*" Proc. Instn. Mech. Engrs. UK, Vol. 203, Part B, 1989, pp.211-216.

[11] Woodham R., "*Photometric method for determining surface orientation from multiple images*", In Shape from Shading, Horn B.K.P., and Brooks M. (Eds.), MIT Press, 1989, pp. 513–532.

[12] Al-Kindi G., Baul R. and Gill K. "*An Example of Automatic Two-Dimensional Component Inspection Using Computer Vision*" Proc. Instn. Mech. Engrs. UK, Vol. 205, Part B, 1991, pp. 241-253.

Table (1) Attribute measurements of investigated objects

(The maximum deviation value of each attribute set resulting from 5 times repetition of the test is recorded)

1.Block gauge component			
Object's attributes	Real value	Computed value	Error
Length (mm)	30	29.3501	0.6499
Width (mm)	9.8	9.3298	0.4702
Height (mm)	10	10.2358	0.2358
2. Tapered shape component			
Object's attributes	Real value	Computed value	Error
Length (mm)	21	20.7921	0.2079
Width (mm)	26	25.8514	0.1486
Height (mm)	30	29.2668	0.7332
3. Cam component			
Object's attributes	Real value	Computed value	Error
Length (mm)	47.7	47.0153	0.6847
Width (mm)	38	38.7291	0.7291
Height (mm)	18.2	17.9426	0.2574
4. Dome shape component			
Object's attributes	Real value	Computed value	Error
Length (mm)	56	55.4596	0.5404
Width (mm)	56	55.6994	0.3006
Height (mm)	29	29.3168	0.3168
5. Rectangular-section rod component			
Object's attributes	Real value	Computed value	Error
Length (mm)	66	66.1104	0.1104
Width (mm)	47	48.4116	0.4116
Height (mm)	53	53.1888	0.1888

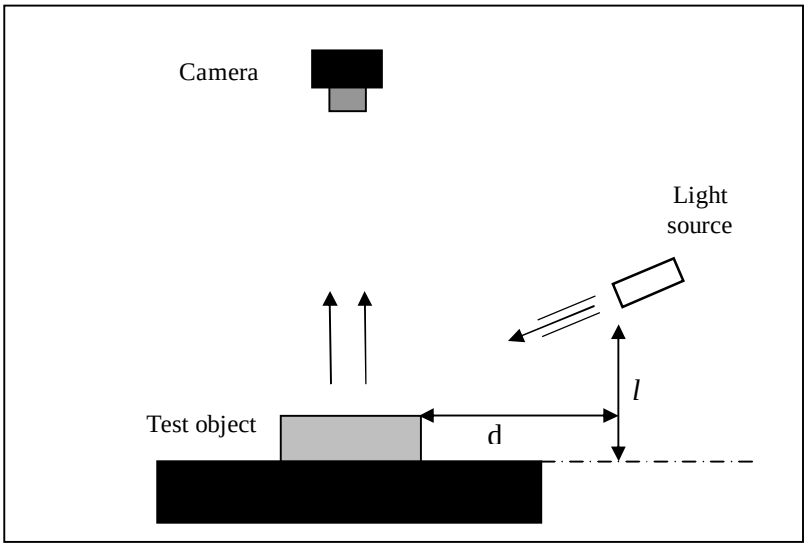

Figure (1) The implemented system set-up

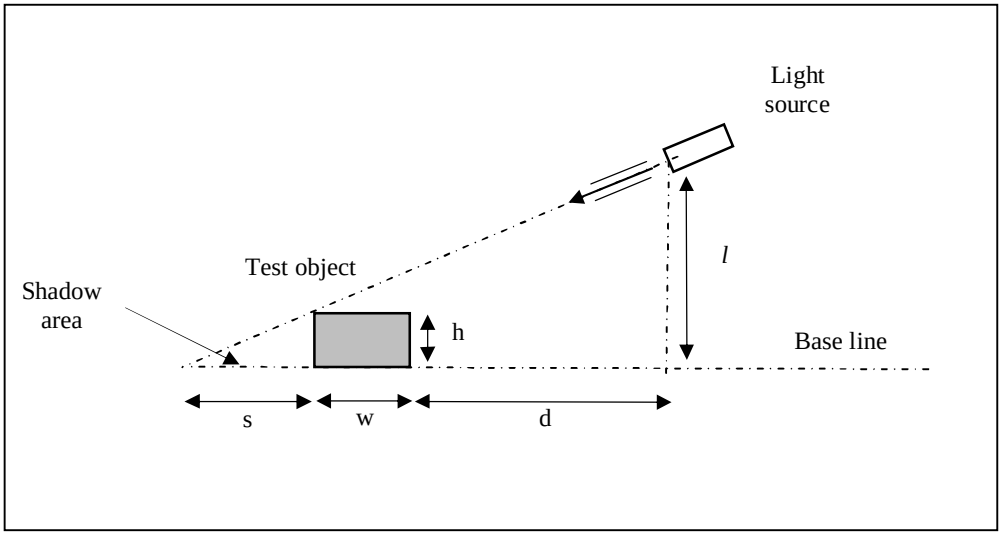

Figure (2) The employed symbols

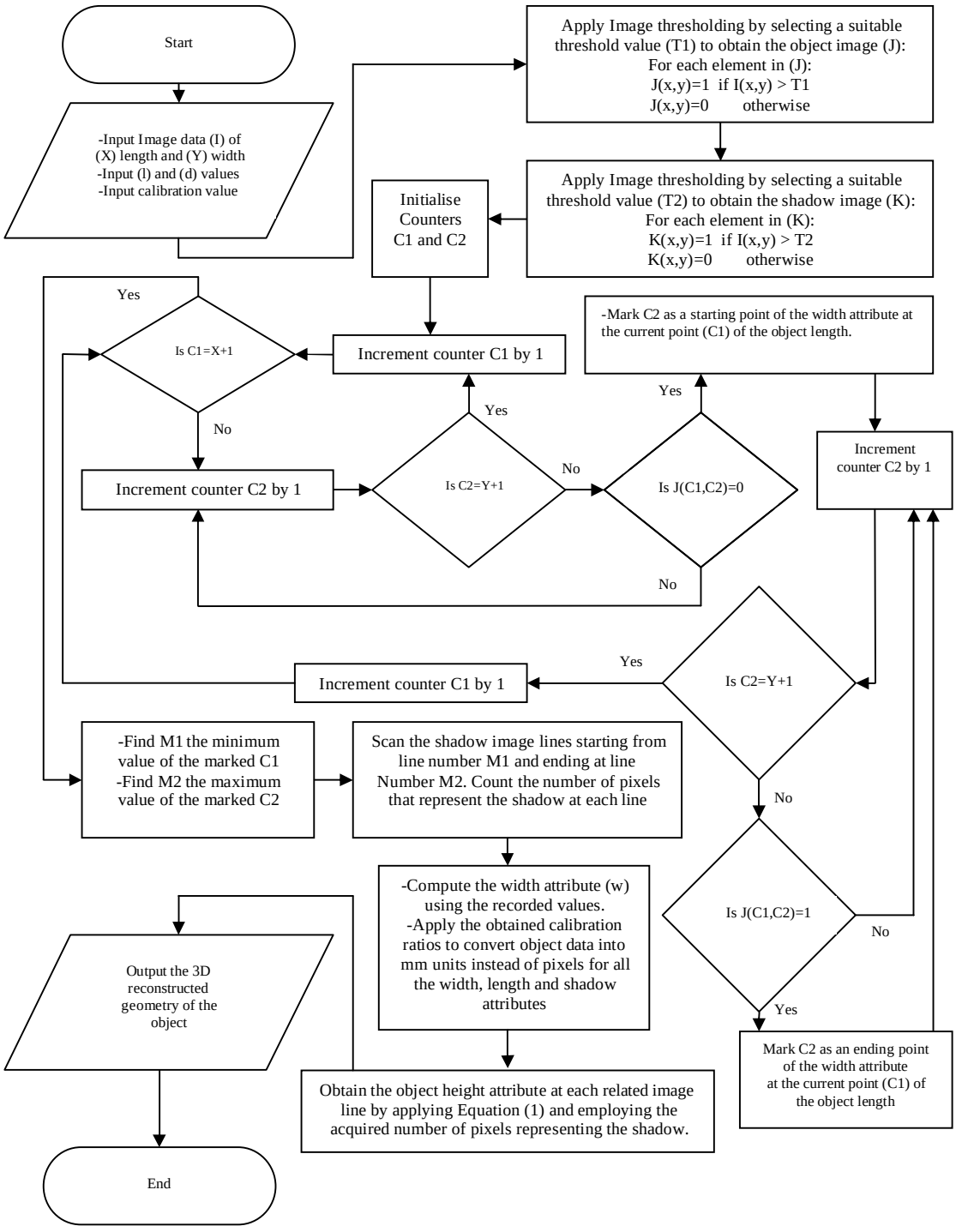

Figure (3) A flow chart of the adopted methodology for 3D object re-construction

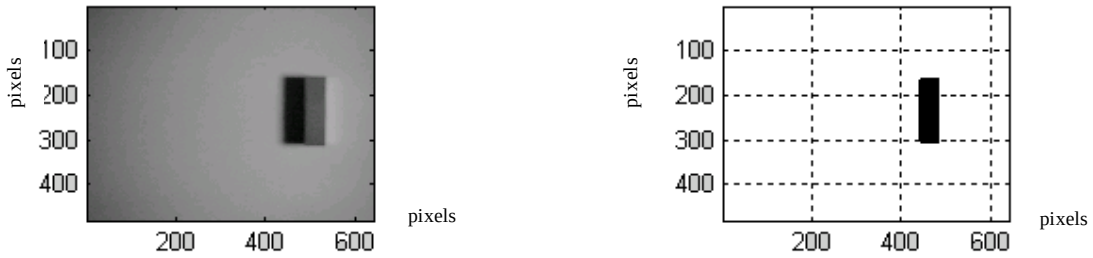

a. Image of block gauge using oblique lighting presentation of the object Shadow

b. Binary

Figure (4) Block Gauge image using oblique lighting

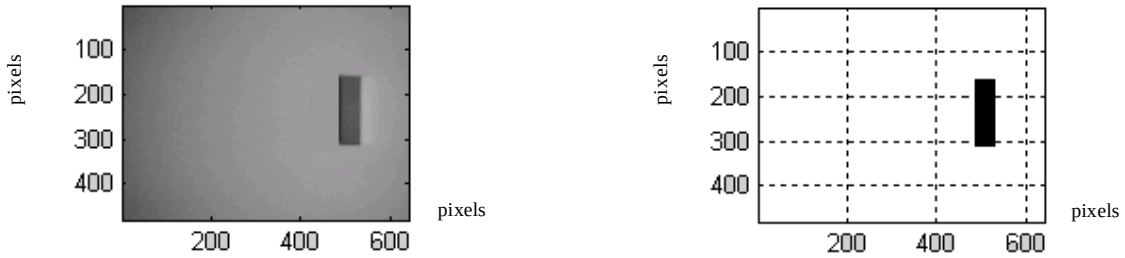

a. Grey scale image of the object

b. Obtained binary image of the object

Figure (5) Block gauge image using ambient lighting

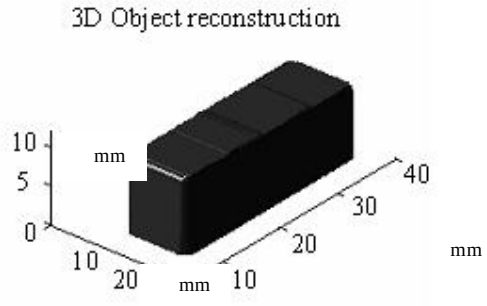

Figure (6) 3D shape re-construction of the block gauge component

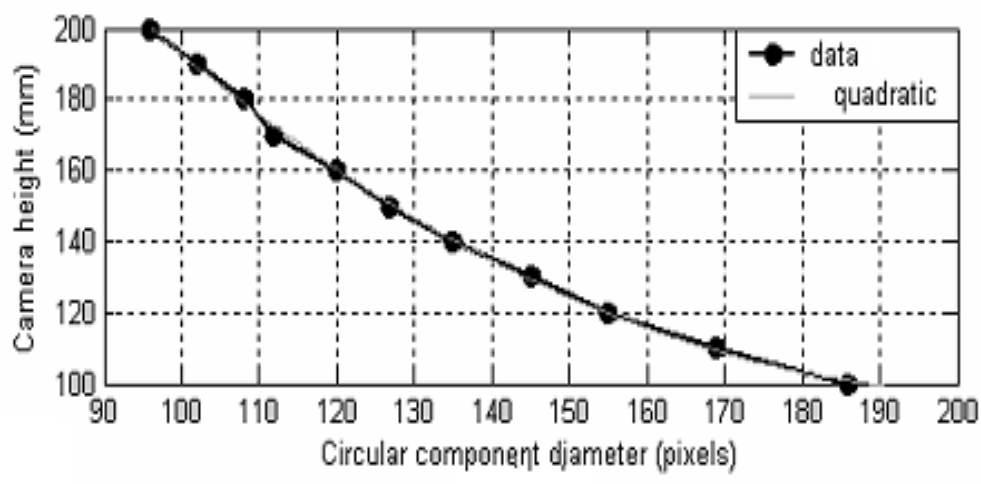

Figure (7) Circular component diameter relationship with camera height

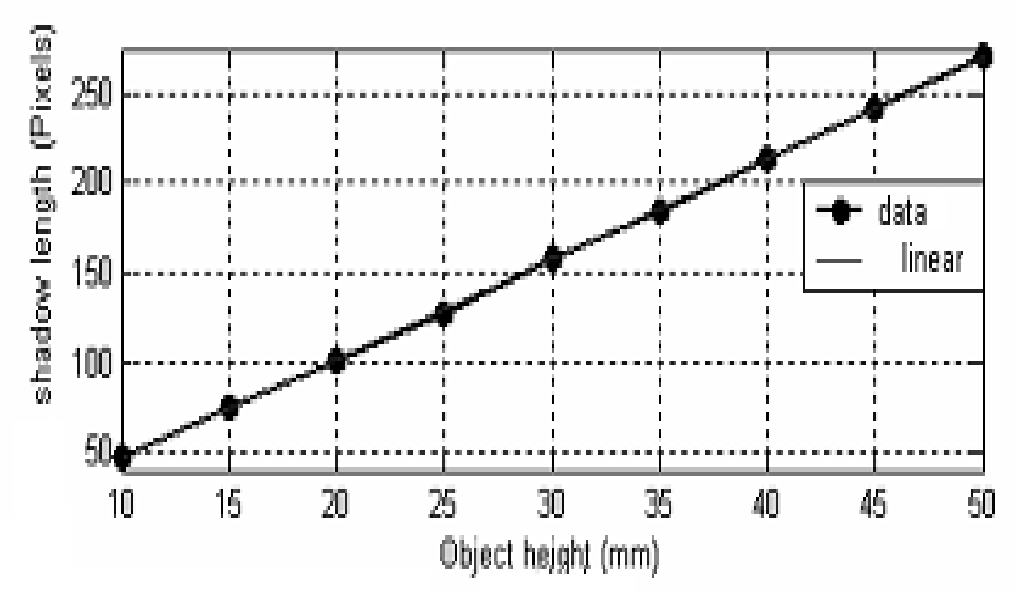

Figure (8) Results of object heights vs. shadow lengths

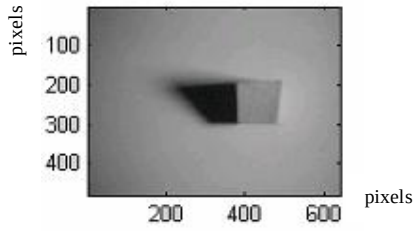

Figure (9) Image of the tapered shape component using oblique lighting

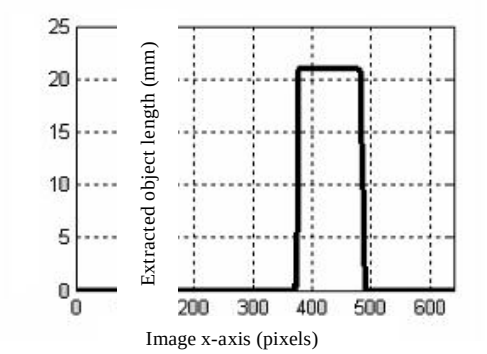

a. Object length attributes

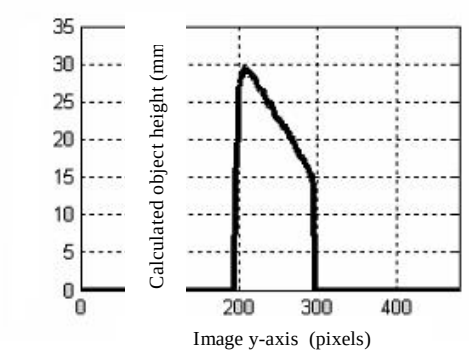

b. Object height attributes

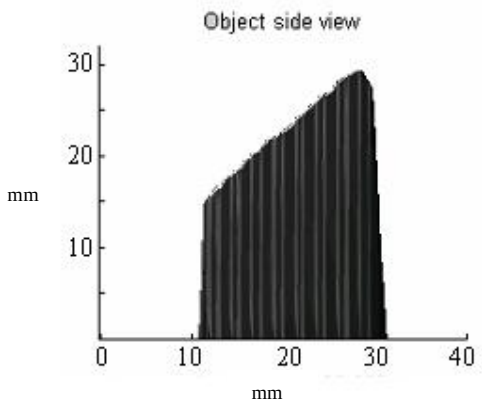

c. Object side view

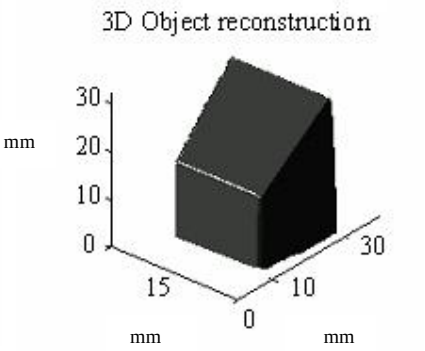

d. 3D object re-construction

Figure (10) 3D shape re-construction of the tapered component

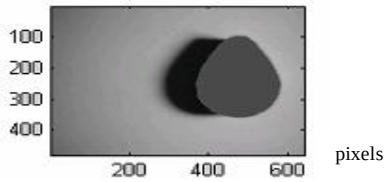

Figure (11) Top view image of the cam component

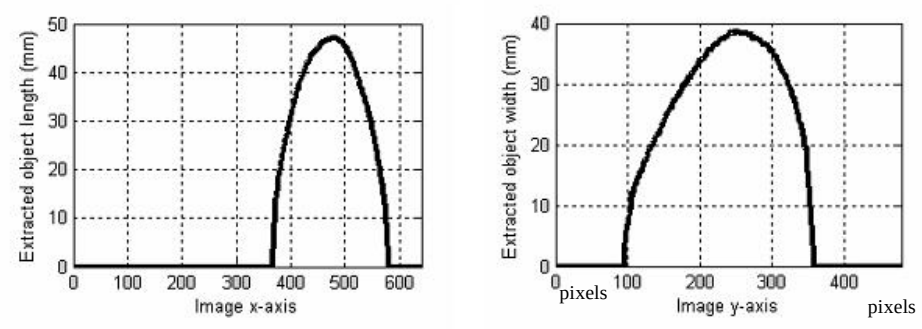

a. Object length attributes

b. Object width attributes

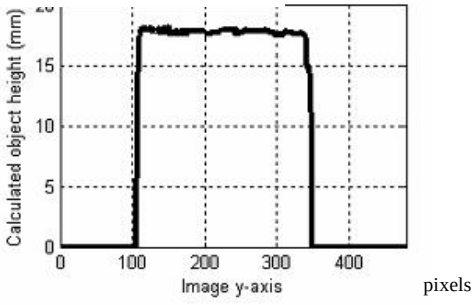

c. Object height attributes

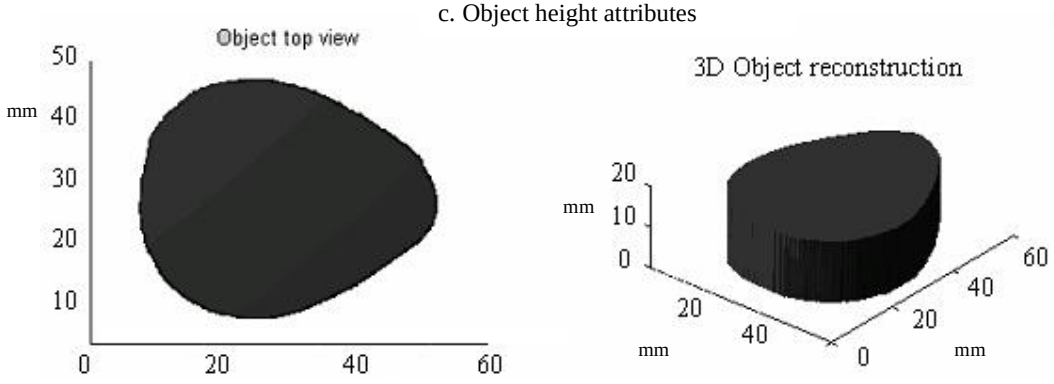

d. Object top view

mm

e. 3D re-construction

Figure (12) 3D shape re-construction of the cam component

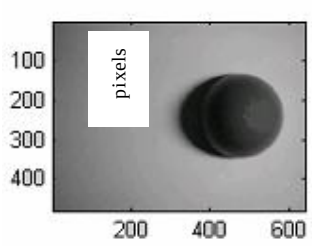

pixels

Figure (13) Top view image of the dome shape component

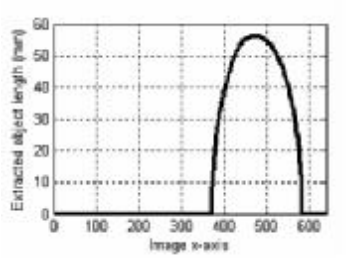

pixels

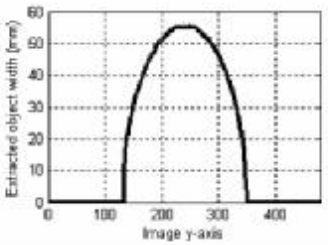

pixels

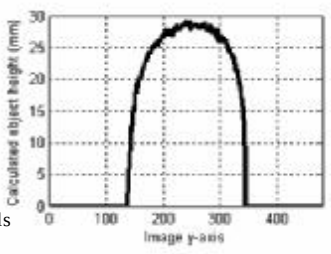

pixels

a. Object length attributes b. Object width attributes c. Object height attributes

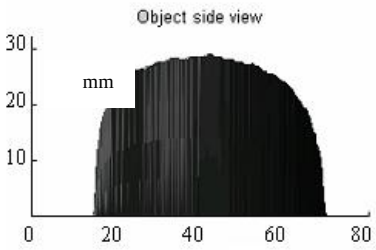

d. Object side view

mm

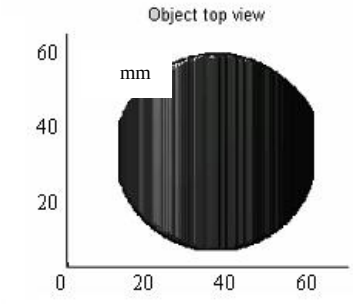

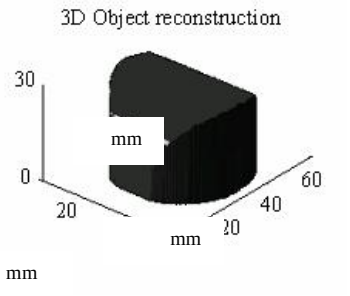

mm

mm

e. Object top view f. 3D re-construction

Figure (14) 3D dome shape component reconstruction detailed views

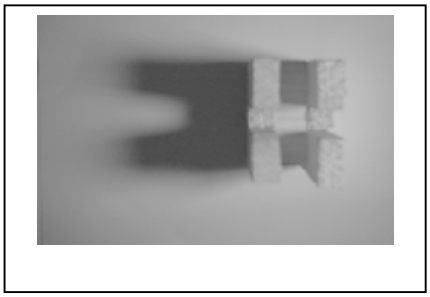

a. Top view image of the rectangular part

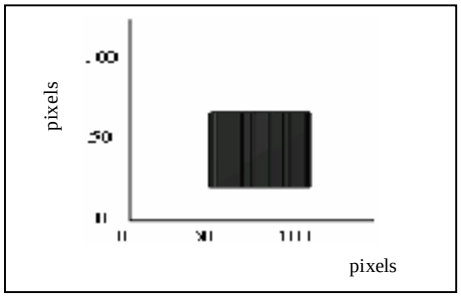

b. Extracted top view of the part

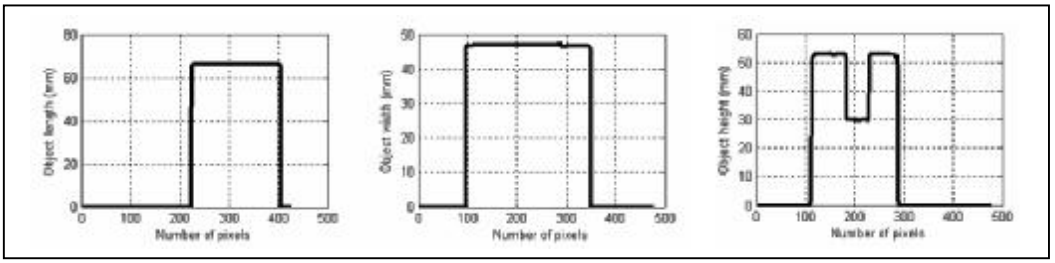

c. Extracted object length, width and height attributes

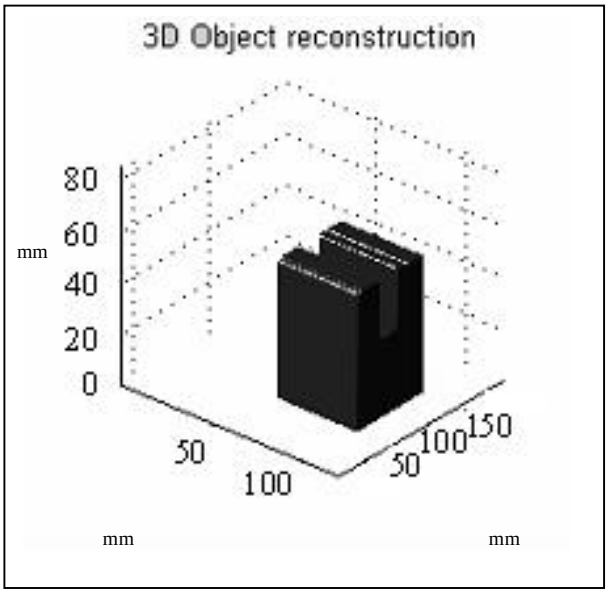

d. 3D re-construction of the part

Figure (15) 3D reconstruction of a block of rectangular section part with perpendicularly crossed deep grooves in its top surface